Complete Location of Poles for Thick Lossy Grounded Dielectric Slab

Swee-Ann Teo, Mook-Seng Leong, *Senior Member, IEEE*, Siou-Teck Chew, *Member, IEEE*, and Ban-Leong Ooi

***Abstract*—In order to obtain accurate closed-form representations of the microstrip Green's functions, it is often necessary to find the locations of the proper and improper surface-wave poles. In this paper, we present an efficient and robust iterative algorithm based on contraction mapping, which can locate all the proper and improper solutions of the characteristics equations of the grounded dielectric slab. The dielectric may also be lossy.**

***Index Terms*—Contraction mapping, Green's function, grounded dielectric slab, improper poles, iterative procedure, microstrip problems, poles and zeros, proper poles, surface-wave poles.**

I. Introduction

VARIOUS analytical and semianalytical techniques have been developed over the past few decades for obtaining closed-form spatial-domain Green's function for microstrip geometry [4]–[8] from the spectral-domain formulation.

In the spectral-domain formulation, the poles of the Green's function for the microstrip correspond to the surface- and leaky-wave modes. In most of these analysis, the extraction of some of these poles is usually required. This is a very important step to derive accurate closed-form Green's functions when the source point is relatively far from the field point.

Recently, with the introduction of new geometries such as low-temperature cofired ceramics (LTCC), it becomes necessary to consider thick substrates, which can support many surface wave modes, thereby highlighting the need to find a technique to extract these poles. Various authors [1], [2] have applied the Newton–Raphson method to the problem, and usually considered only the case where the substrate is lossless.

However, for substrates that are thick and lossy, it may be difficult to provide suitable initial guesses for some of the poles, especially those that may lie very close to one another.

Gugliemi and Jackson [3] have used an asymptotic method that is only valid for low-frequency approximations.

In this paper, a systematic algorithm that can locate all the surface- and leaky-wave poles is proposed.

The proposed algorithm is based on a well-known technique in functional analysis, known as "contraction mapping." We shall also prove the completeness of this method and, hence, show that the location of all the poles (proper and improper) of such a Green's function can be found using this method. The substrate is assumed to be lossy.

Manuscript received November 22, 2000. This work was supported by the National University of Singapore and the RF Laboratory of the DSO National Laboratories, Singapore.

The authors are with the Microwave Division, Department of Electrical and Computer Engineering, National University of Singapore, Singapore 119260.

Publisher Item Identifier S 0018-9480(02)01157-2.

II. Theory

The following theorems to be introduced will form the basis of the proof of convergence and completeness of the proposed algorithm.

Theorem 1 (Fixed Point Theorem): Let $\mathcal{M}$ be a mapping of any metric space R into itself. z_f is then called a fixed point of $\mathcal{M}$ in R if it satisfies the following equation [9]:

$$z_f = \mathcal{M}z_f. \tag{1}$$

If $\mathcal{M}$ has the additional property that for any $z_1,\, z_2 \in R$

$$|\mathcal{M}z_1 - \mathcal{M}z_2| < |z_1 - z_2| \tag{2}$$

then $\mathcal{M}$ is known as a contraction mapping, and will always have one and only one fixed point. This technique is often called the method of successive approximations.

In general, if $\mathcal{M}$ is a contraction mapping with domain R, the solution of $z = \mathcal{M}z$ is given by

$$z_f = \lim_{n\to\infty} \mathcal{M}^n z_0 \tag{3}$$

where z_0 is any point in S.

Theorem 2: If $\mathcal{M}$ is a continuous mapping in a metric space R that maps *into itself*, then it is a contraction mapping if its first derivative exists and has a magnitude of less than unity throughout the region R, i.e.,

$$\left|\frac{\partial(\mathcal{M}z)}{\partial z}\right| < 1, \qquad \text{for all } z \in R. \tag{4}$$

This theorem can be proved by noting that any line transformed by such a mapping will have a shorter length if the above condition is satisfied.

Theorem 3: Let $\mathcal{M}$ be a continuous function that satisfies the following:

$$\left|\frac{\partial \mathcal{M}x}{\partial x}\right| < 1, \qquad x \in R^+ \tag{5}$$

$$\left|\frac{\partial \mathcal{M}x}{\partial x}\right| \geq 1, \qquad x \in R^-. \tag{6}$$

The inverse operator $\mathcal{M}^{-1}$, if it exists, will then satisfy the following:

$$\left|\frac{\partial \mathcal{M}^{-1}x}{\partial x}\right| \leq 1, \qquad x \in \mathcal{M}R^-. \tag{7}$$

If $\mathcal{M}$ has a fixed point x_0, then there must exist an ε neighborhood N_ε of x_0 such that

$$\lim_{n\to\infty} \mathcal{M}^n x = x_0, \qquad x \in N_\varepsilon$$

or

$$\lim_{n\to\infty} \mathcal{M}^{-n} x = x_0, \qquad x \in N_\varepsilon.$$

Proof: Suppose that there does not exist such a neighborhood. Then

$$|\mathcal{M}(z_0+\delta z) - z_0| > |\delta z| \Rightarrow \left|\frac{\partial \mathcal{M} z_0}{\partial z}\right| > 1 \tag{8}$$

and

$$|\mathcal{M}^{-1}(z_0+\delta z) - z_0| > |\delta z| \Rightarrow \left|\frac{\partial \mathcal{M}^{-1} z_0}{\partial z}\right| > 1. \tag{9}$$

Due to (8), $z_0 \in R^-$, and due to (9), $z_0 \notin \mathcal{M}R^-$. However, since $\mathcal{M}z_0 = z_0$, $z_0 \in \mathcal{M}R^-$. Hence, a contradiction results. ■

It follows from this theorem that, if there exist a fixed point for $\mathcal{M}$ in R, then at least one of the operator $\mathcal{M}$ or $\mathcal{M}^{-1}$ must be convergent to the fixed point, about an ε neighborhood of the fixed point.

Theorem 4 (Continuity of Solutions): The set solutions of the characteristics equations, including those in the second Riemann sheet, is a continuous function of all the parameters, except at possibly discrete points.

The can be shown by rewriting the characteristics equation into the following form:

$$f(x_K, K) = x_K$$

where K can be any one of the parameters and x_K is a solution of the characteristics equation. It is known that the function f is analytic in terms of x and K, and if the second Riemann sheet is included, then there is no branch cut in the function. Therefore, since f is also a bounded function of x and K as follows:

$$\begin{aligned}\frac{\partial x_K}{\partial K} &= \frac{\partial f(x_K, K)}{\partial K}\\ &= \frac{\partial f(x_K, K)}{\partial x}\frac{\partial x_K}{\partial K} + \frac{\partial f(x_K, K)}{\partial K}\\ &= \frac{\partial f(x_K, K)}{\partial K}\left(1 - \frac{\partial f(x_K, K)}{\partial x}\right)^{-1}\end{aligned}$$

unless $\partial f(x_K, K)/\partial x = 1$, $|\partial x_K/\partial K|$ will also be bounded.

When $\partial f(x_K, K)/\partial x = 1$, x_K corresponds to a pole of degree 2 or higher. If $\partial^2 f(x_K, K)/\partial x^2 \neq 0$, then x_K is a pole of degree 2 only, and can only happen at discrete points of K and x. Fortunately this does not pose a problem as K is, in general, a complex value and we can deform the path of K around this point.

III. TE Modes

The characteristic equation for the TE mode, in a grounded dielectric slab, is given by

$$u_2 \cosh u_2 h \pm u_1 \sinh u_2 h = 0 \tag{10}$$

where

$$u_1 = \sqrt{k_r^2 - k_0^2} \tag{11}$$

$$u_2 = \sqrt{k_r^2 - k_0^2 \varepsilon_r} \tag{12}$$

h is the thickness of the substrate and ε_r is the complex relative permittivity of the substrate.

As the zeros of the above equation is independent of the branch of u_2 selected, we can make the substitution $w = u_2 h$ to obtain

$$w^2 = K^2 \sinh^2 w \tag{13}$$

where

$$K = k_0 h \sqrt{\varepsilon_r - 1}. \tag{14}$$

Hence, taking square root of the components, we obtain for the two branches

$$w = \pm K \sinh w. \tag{15}$$

Taking the inverse of (15), we obtain

$$w = \pm \operatorname{arcsinh} \frac{w}{K}. \tag{16}$$

By a careful analysis of the way the functions are mapped by the arcsinh function, we postulate that the solutions can be obtained by constructing contraction mappings out of each different branch of the function such that the fixed points of these mappings are the solution of the characteristics equation. The mappings are classified into the following four main categories.

Case 1:

$$\mathcal{L}_1 w = \operatorname{arcsinh} \frac{w}{K} \tag{17}$$

$$\operatorname{Re}[\mathcal{L}_1 w] \geq 0 \tag{18}$$

$$2m\pi < \operatorname{Im}[\mathcal{L}_1 w] \leq (2m+1)\pi. \tag{19}$$

Case 2:

$$\mathcal{L}_2 w = \operatorname{arcsinh} \frac{w}{K} \tag{20}$$

$$\operatorname{Re}[\mathcal{L}_2 w] \leq 0 \tag{21}$$

$$\left(2m + \tfrac{3}{2}\right)\pi < \operatorname{Im}[\mathcal{L}_2 w] \leq \left(2m + \frac{5}{2}\right)\pi. \tag{22}$$

Case 3:

$$\mathcal{L}_3 w = -\operatorname{arcsinh} \frac{w}{K} \tag{23}$$

$$\operatorname{Re}[\mathcal{L}_3 w] \geq 0 \tag{24}$$

$$(2m+1)\pi < \operatorname{Im}[\mathcal{L}_3 w] \leq (2m+2)\pi. \tag{25}$$

Case 4:

$$\mathcal{L}_4 w = -\operatorname{arcsinh} \frac{w}{K} \tag{26}$$

$$\operatorname{Re}[\mathcal{L}_4 w] \leq 0 \tag{27}$$

$$\left(2m + \frac{1}{2}\right)\pi < \operatorname{Im}[\mathcal{L}_4 w] \leq \left(2m + \frac{3}{2}\right)\pi \tag{28}$$

where m is any nonnegative integer. Negative values of m are not considered, as they are a repetition of the solutions for positive m, except for a change of sign. The trivial pole at $w = 0$ is also not considered and it corresponds to $m = -1$ for case 2.

Special care must be taken when w/K is an imaginary quantity. In this case, there might be some ambiguity over the selection of the two possible branches available in the mapping. By

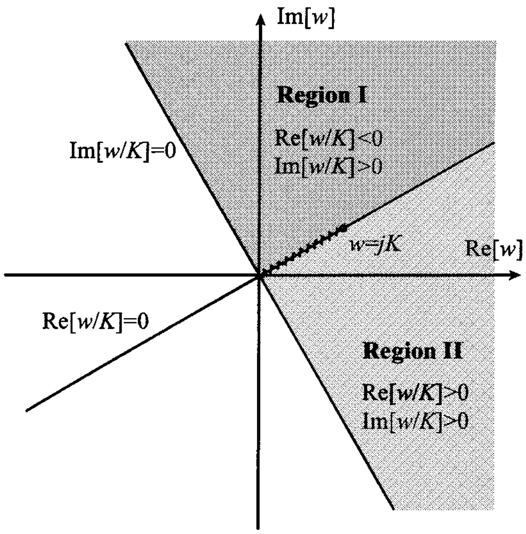

Fig. 1. Possible definition of a domain for $\mathcal{L}_1$.

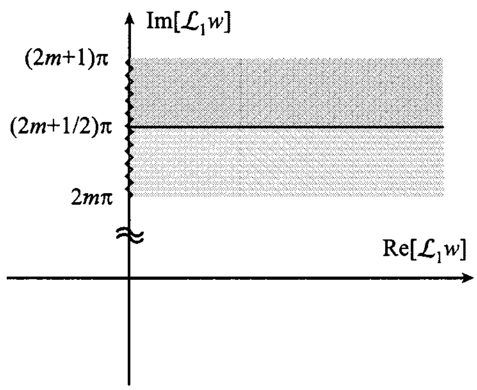

Fig. 2. Range and domain of $\mathcal{L}_1$ for a specific value of m.

taking the limits, it is found that the branch of $\mathcal{L}_1$ with a larger imaginary part should be chosen.

As an example, choosing $K = 20$, and constructing the series $\{w_{n+1} = \mathcal{L}_1 w_n, n \geq 0 | w_0 = j\}$ for $m = 1$, we obtain

$$\begin{aligned} w_0 &= j \\ w_1 &= 9.40648j \\ w_2 &= 9.2518j \\ w_3 &= 9.25468j \\ w_4 &= 9.25462j \\ &\vdots \end{aligned}$$

IV. Convergence of TE Operator

The only question that remains now is when the mappings are convergent. In this section, the conditions that are required for the convergence of these operators are derived. In some instances, the operators might be nonconvergent, and some modifications are to be made.

For brevity, only the part of the proof for $\mathcal{L}_1$ will be presented. The other cases are to be handled in a similar manner.

If the domain of the operator $\mathcal{L}_1$ is defined to be the shaded area in Fig. 1, then the range of $\mathcal{L}_1$ is as shown in Fig. 2. However, to be concurrent with the definition of a contraction mapping, both the domain and range shall be set to be the same, as shown in Fig. 2, or as follows:

$$\mathrm{Re}[w] \geq 0 \tag{29}$$

$$2m\pi < \mathrm{Im}[w] \leq (2m+1)\pi. \tag{30}$$

It should be noted that there is a line of discontinuity in the domain of the problem, which is the straight line between $w = 0$ and $w = jK$. It is shown as the jagged line in Fig. 1.

When $2m\pi > \mathrm{Im}[jK]$, then there is no discontinuity in the domain of $\mathcal{L}_1$. As such, as stated by theorem 2, the condition required for $\mathcal{L}_1$ to be a contraction mapping is simply

$$\left|\frac{\partial \mathcal{L}_1}{\partial w}\right| = \left|\frac{1}{\sqrt{K^2 + w^2}}\right| < 1. \tag{31}$$

It is clear that, if this condition is satisfied, then the operator can have one and only one unique fixed point due to theorem 1.

The next portion of the complex plane to be considered is the part where the domain of $\mathcal{L}_1$ contains part of the discontinuity (jagged line in Fig. 1), but still satisfies (31).

In this case, the domain of $\mathcal{L}_1$ is divided into two separate regions by this line of discontinuity. Fortunately, it can be shown that there will be no solution to the right of the discontinuity.

By restricting the domain to the portion bounded by the imaginary axis and the discontinuity, a contraction mapping that is totally continuous is obtained again. Hence, a fixed point will be found within this region. It follows that if K is a real number, then the solution w must lie on the imaginary axis.

We have now shown that when the $\mathcal{L}_1$ satisfies (31), it is always convergent, and has one and only one unique fixed point.

To analyze the case where the operator does not satisfy (31), contraction mappings alone will not be adequate. First, by using theorem 4, it can be shown that the solutions of the characteristic equation must be continuous with respect to K, and that there can only be one solution corresponding to each operator.

Therefore, due to theorem 3, at least one of the operator, i.e., $\mathcal{L}_1$ or $\mathcal{L}_1^{-1}$, must be convergent to the location of the fixed point. In general, only $\mathcal{L}_1$ or $\mathcal{L}_3$ might require the use of the inverse operator. The other operators $\mathcal{L}_2$ and $\mathcal{L}_4$ are always convergent.

For $\mathcal{L}_1$ and $\mathcal{L}_3$, the ε neighborhood of convergence of the forward and inverse operators may be very small when (31) is not satisfied; in order to resolve this, the operator is modified slightly. It is to be used when $\mathcal{L}_i$ is nonconvergent as follows:

$$\mathcal{L}_i' w = \frac{\mathcal{L}_i^{-1} w + w}{2}. \tag{32}$$

The reason for this operator is due to theorem 3. When this operator is used, the initial starting point should be $w = jK$.

If the above operator is also nonconvergent, then the following operator is to be used as follows:

$$\mathcal{L}_i'' w = \frac{\mathcal{L}_i w + w}{2}. \tag{33}$$

It can be seen that the condition for the convergence of the above operator is

$$\left|\frac{\partial \mathcal{L}'}{\partial w}\right| = \left|\frac{1}{2\sqrt{K^2 + w^2}} + \frac{1}{2}\right| < 1 \tag{34}$$

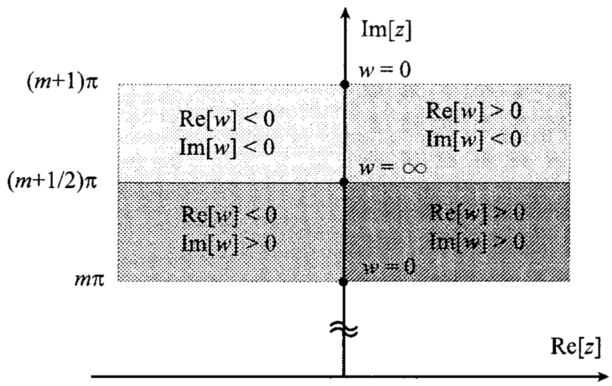

Fig. 3. Behavior of $w = \tanh z$.

which is a less stringent condition than (31).

The reason for this apparent convoluted chain of operator is due to numerical considerations, rather than for any theoretical reason.

In conclusion, using a combination of the mappings, all the poles associated with the TE characteristics equation can be located. Completeness of the solution is also shown.

V. TM Modes

In this section, a similar algorithm for the TM modes is presented. The algorithm is more complex as the characteristics equation now depends on two parameters rather than one. There is also similar discontinuity in the mapping, which depends on how the branch cut is chosen in the complex plane.

The TM characteristics equation is given by

$$\varepsilon_r u_1 \cosh u_2 h \pm u_2 \sinh u_2 h = 0. \tag{35}$$

By means of the substitution $w = u_2 h$, we obtain the following, which forms the basis of the operators:

$$w = \operatorname{arctanh} \frac{\varepsilon_r \sqrt{w^2 + K^2}}{w} \tag{36}$$

where $K = k_0 h \sqrt{\varepsilon_r - 1}$.

By differentiating the above expression, it is shown that the convergence of operators based on the above is affected by following points:

$$w_a = \pm \frac{jk_0 h \varepsilon_r}{\sqrt{1+\varepsilon_r}} = \pm jk_0 h \sqrt{(\varepsilon_r - 1) + \frac{1}{1+\varepsilon_r}} \tag{37}$$

$$w_b = \pm jk_0 h \sqrt{\varepsilon_r - 1}. \tag{38}$$

It is noted that the two points may be very close together if ε_r is large.

By making use of the following property:

$$\tanh(\alpha + j\beta) = \frac{\sinh 2a + j \sin 2\beta}{\cosh 2a + \cos 2\beta} \tag{39}$$

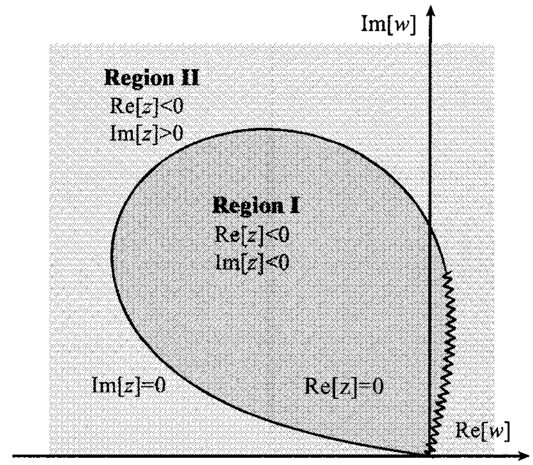

Fig. 4. Selection of branch cut and largest possible definition of a domain for $\mathcal{K}_1$.

a map of the tanh function can be drawn. Fig. 3 shows how the arctanh function maps the different regions of the complex plane onto itself. For instance, by selecting the appropriate branch of the mapping, the second quadrant of the complex plane is mapped by arctanh into the region described by the following:

$$\operatorname{Re}[z] \le 0$$
$$m\pi \le \operatorname{Im}[z] \le \left(m + \frac{1}{2}\right)\pi.$$

A. Type-I TM Mapping

The first group of solutions are those that are in the second quadrant. In order to avoid any discontinuity of the mapping in the second quadrant, the branch cut is the jagged line, as shown in Fig. 4, and the branch of the square root is the one where the results have a negative real part. This ensures that the result of taking arctanh also has a negative real part and is confined to the second quadrant. Therefore, the first operator is as follows:

Case 1:

$$\mathcal{K}_1 w = \operatorname{arctanh} \frac{\varepsilon_r \sqrt{w^2 + K^2}}{w} \tag{40}$$

$$\operatorname{Re}\left[\frac{\varepsilon_r \sqrt{w^2 + K^2}}{w}\right] \le 0 \tag{41}$$

$$m\pi < \operatorname{Im}[\mathcal{K}_1 w] \le (m+1)\pi. \tag{42}$$

Since the mapping is continuous (by theorem 2), the only condition required for the mapping to be a contraction mapping is

$$\left|\frac{\partial \mathcal{K}_1 w}{\partial w}\right| = \left|\frac{K^2 \varepsilon_r}{\sqrt{K^2 + w^2}\left[K^2 \varepsilon_r^2 + w^2(\varepsilon_r^2 - 1)\right]}\right| < 1. \tag{43}$$

Hence, when (43) is satisfied, a contraction mapping is obtained, and by theorem 1, each mapping will have a unique fixed point.

B. Type-II TM Mapping

Case 2:

$$\mathcal{K}_2 w = \operatorname{arctanh} \frac{\varepsilon_r \sqrt{w^2 + K^2}}{w} \tag{44}$$

$$\operatorname{Im}\left[\frac{\varepsilon_r \sqrt{w^2 + K^2}}{w}\right] \geq 0 \tag{45}$$

$$m\pi < \operatorname{Im}[\mathcal{K}_2 w] \leq \left(m + \frac{1}{2}\right)\pi. \tag{46}$$

This operator is to be used when its domain includes the jagged line shown in Fig. 4 and (43) is satisfied. Due to the selection of the branch of the square root, as defined in the operator itself, the line where $\operatorname{Im}[z] = 0$ is now selected as the branch cut. Although there is a discontinuity in the mapping, there is no ambiguity because there is no solution in the second quadrant for this operator. In fact, the solution lies in the narrow strip bounded by the jagged line and the imaginary axis. It follows that, if ε_r is a real number, the solution w must lie on the imaginary axis.

When the jagged line is no longer included in the domain of this operator, the operator does not have a solution. The next operator $\mathcal{K}_3$ to be introduced should be used instead.

C. Type-III TM Mapping

Case 3:

$$\mathcal{K}_3 w = \operatorname{arctanh} \frac{\varepsilon_r \sqrt{w^2 + K^2}}{w} \tag{47}$$

$$\operatorname{Re}\left[\frac{\varepsilon_r \sqrt{w^2 + K^2}}{w}\right] \geq 0 \tag{48}$$

$$\left(m + \frac{1}{2}\right)\pi < \operatorname{Im}[\mathcal{K}_3 w] \leq (m+1)\pi. \tag{49}$$

For this operator, the starting point should be $w = [j(m + (3/4))\pi + Q]$, where Q is a sufficiently large number such that w is away from w_a and w_b and is in region II of Fig. 4.

This operator is a complement of the previous operator. When $\mathcal{K}_2$ cannot be used, as its domain does not include the jagged line shown in Fig. 4, $\mathcal{K}_3$ should be used.

When the domains of the operators do not satisfy (43), the operators are to be modified as their ε neighborhood of convergence may be small. The following operators are to be used:

$$\mathcal{K}_i' w = \frac{\mathcal{K}_i w + w}{2}. \tag{50}$$

It should be noted that, in the vicinity of w_a and w_b, both operators 2 and 3 will have solutions. If $\mathcal{K}_3'$ does not converge, then the inverse operator should be used as follows:

$$\mathcal{K}_3'' w = \frac{\sqrt{w^2 \tanh^2 w - K^2 \varepsilon_r^2}}{\varepsilon_r} \tag{51}$$

$$\operatorname{Re}[\mathcal{K}_3'' w] \geq 0. \tag{52}$$

The use of the inverse operator is similar to that of the TE case. The proof of the completeness of the solutions for the TM characteristics equation can be similarly constructed. Where (43) is satisfied, theorems 1 and 2 are used to show the uniqueness of the solutions. When the condition is not satisfied, theorems 3 and 4 are then to be used.

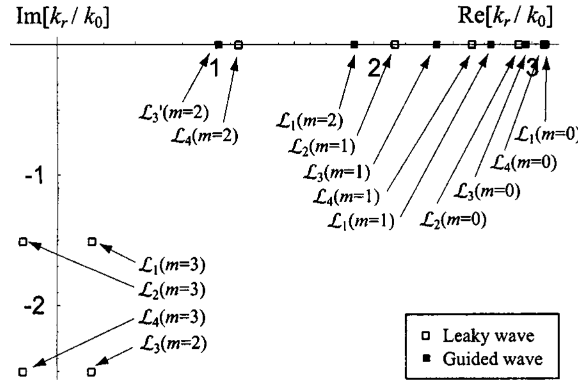

Fig. 5. Location of TE poles for 10 GHz ($h = 0.028$ and $\varepsilon_r = 9.8$) showing the use of the $\mathcal{L}_3'$ operator for $m = 2$.

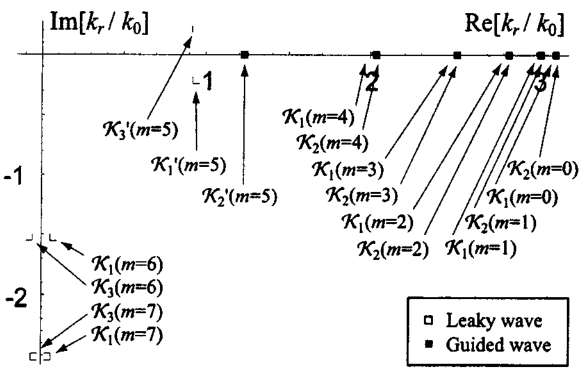

Fig. 6. Locations of TM poles for 10 GHz ($h = 0.028$ and $\varepsilon_r = 9.8$).

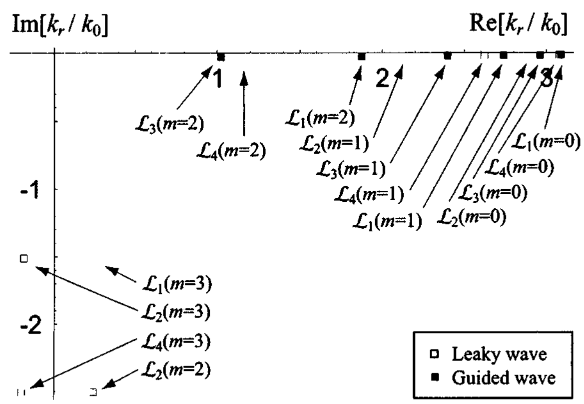

Fig. 7. Location of TE poles for 10 GHz ($h = 0.028$ and $\varepsilon_r = 9.8 - j0.1$).

VI. Numerical Results

In this section, some numerical results are presented. The algorithm was able to extract the poles for both the TE and TM poles using a negligible amount of computing time.

All the poles shown in these examples are extracted in less than 1 s on a Pentium II 233-MHz computer. The algorithm was programmed using Mathematica.

As are shown in Figs. 5 and 6, when the dielectric is losses, the poles are purely real. When the some losses were introduced, the poles will migrate lower down the complex plane, as shown in Figs. 7 and 8. Note that, in the example, as shown in Fig. 5, the operator $\mathcal{L}_2$ does not converge for $m = 2$ and, hence, the operator $\mathcal{L}_2'$ was used.

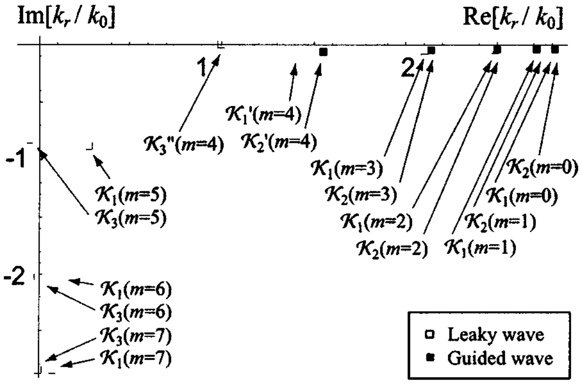

Fig. 8. Location of TM poles for 10 GHz ($h = 0.028$ and $\varepsilon_r = 8 - j0.2$) showing the use of the $\mathcal{K}_3''$ operator for $m = 4$.

VII. Conclusion

In this paper, we have demonstrated the use of the method of successive approximations or contraction mapping to locate the solutions of characteristics equations of microstrip structures.

The usefulness of this technique lies in the proof of the existence and uniqueness of the solutions. This will facilitate the use of techniques based on Cauchy's residue theorem to evaluate the Sommerfeld integral.

An application of this algorithm would be for deriving closed-form spatial-domain Green's function using the discrete complex image method (DCIM). It is known that the accuracy of the Green's functions derived using the DCIM in the far-field region depends on whether all the guided wave poles have been extracted.

The algorithm is also able to overcome the difficulties associated with the extraction of pairs of poles that are sometimes located very close to each other.

References

[1] C. G. Hsu, R. F. Harrington, J. R. Mautz, and T. K. Sarkar, "On the location of leaky wave poles for a grounded dielectric slab," *IEEE Trans. Microwave Theory Tech.*, vol. 39, pp. 346–349, Feb. 1991.

[2] M. A. Martin, S. Barkeshli, and P. H. Pathak, "On the location of proper and improper surface wave poles for the grounded dielectric slab," *IEEE Trans. Antennas Propagat.*, vol. 38, pp. 570–573, Apr. 1990.

[3] M. Gugliemi and D. R. Jackson, "Low-frequency location of the leaky-wave poles for a dielectric layer," *IEEE Trans. Microwave Theory Tech.*, vol. 38, pp. 1743–1746, Nov. 1990.

[4] S. Barkeshli, P. H. Pathak, and M. Martin, "An asymptotic closed-form microstrip surface Green's function for the efficient moment method analysis of mutual coupling in microstrip antennas," *IEEE Trans. Antennas Propagat.*, vol. 38, pp. 1374–1382, Sept. 1990.

[5] S. Q. Li, L. Tsang, and C. G. Huang, "Closed-form spatial electric field Green's functions of microstrip structures using the fast Hankel transform and the matrix pencil method," *Proc. Inst. Elect. Eng.*, vol. 147, pp. 161–166, June 2000.

[6] G. Dural and M. I. Aksun, "Closed-form Green's functions for general sources and stratified media," *IEEE Trans. Microwave Theory Tech.*, vol. 43, pp. 1545–1552, July 1995.

[7] Y. L. Chow, J. J. Yang, D. G. Fang, and G. E. Howard, "A closed-form spatial Green's function for the thick microstrip substrate," *IEEE Trans. Microwave Theory Tech.*, vol. 39, pp. 588–592, Mar. 1991.

[8] W. C. Chew, *Waves and Fields in Inhomogeneous Media*. New York: Van Nostrand, 1990, ch. 2.

[9] A. N. Kolmogorov and S. V. Fomin, *Introductory Real Analysis*. New York: Dover, 1970.

[10] R. W. Hamming, *Numerical Methods for Scientists and Engineers*. New York: Dover, 1973.

Swee-Ann Teo received the B.Eng. degree (with honors) in electrical engineering from the National University of Singapore, Singapore, in 1999, and is currently working toward the M.Eng. degree from the National University of Singapore.

He is currently with the National University of Singapore, where he is a Research Scholar. He is currently with the Wireless Connectivity Division, Microtune Inc., as an RFIC Engineer. His main research interests includes integral-equation methods, fast multipole methods, and discrete complex image methods.

Mook-Seng Leong (M'75–SM'98) received the B.Sc. degree in engineering (first-class honors) and the Ph.D. degree in microwave engineering from the University of London, London, U.K., in 1968 and 1971, respectively.

From 1971 to 1973, he was a Post-Doctoral Research Fellow at Queen Mary College, London University, where he investigated high-efficiency microwave antennas in collaboration with Andrew Antennas and Microwave Associates. In 1973, he joined the National University of Singapore, Singapore, as a Professor and Head of the Microwave and RF Group, Electrical and Computer Engineering Department. He has authored or co-authored over 150 technical papers in international journals and has been consulted extensively by statutory boards and public and private companies. He co-authored the textbook *Spheroidal Wave Functions in Electromagnetic Theory* (New York: Wiley). He has published over 150 technical papers in international journals and has been consulted extensively by statutory boards, public and private companies. His current research interests are electromagnetic-wave propagation and scattering, antenna design and analysis, and electromagnetic compatibility. He is an Editorial Board Member of *Microwave and Optical Technology Letters* and *Wireless Personal Communications*.

Dr. Leong is a member of the Massachusetts Institute of Technology (MIT)-based Electromagnetics Academy and a Fellow Member of the Institute of Electrical Engineers (IEE), U.K. He is the founder chairman of the Singapore IEEE Microwave Theory and Techniques (MTT)/Antennas and Propagation (AP) Chapter.

Siou-Teck Chew (S'94–M'96) received the B. Eng. degree (with honors) and M. Eng. degree from the National University of Singapore (NUS), Singapore, in 1989 and 1993, respectively, and the Ph.D. degree from the University of California at Los Angeles (UCLA), in 1996.

Since 1989, he has been with the DSO National Laboratories, Singapore, where he is currently the Centre Head (Advanced Electronics and Signal Processing) and Distinguished Member of Technical Staff. He oversees the research and development of digital and microwave components and subsystems and advanced signal processing. He is also currently an Adjunct Associate Professor at NUS, where he lectures and supervises research activities. His technical interests include active antennas, high power amplifiers, filters, and nonlinear circuit analysis and design. He has authored or co-authored 20 papers and one book.

Dr. Chew is the chairman of the IEEE Singapore Chapter for Antennas and Propagation (AP)/Microwave Theory and Techniques (MTT)/Electromagnetic Compatibility (EMC) (2000-2001). He was the recipient of a DTTA Scholarship presented by the Ministry of Defence, Singapore.

Ban-Leong Ooi received the B.Eng. and Ph.D. degrees from the National University of Singapore, Singapore, in 1992 and 1997, respectively.

He is currently an Assistant Professor in the Department of Electrical and Computer Engineering, National University of Singapore. His main research interests include active antennas, microwave semiconductor device modeling and characterization, package modeling, microwave and millimeter-wave circuits, and electromagnetic numerical methods.

Dr. Ooi was the Singapore IEEE Microwave Theory and Techniques (MTT)/Electromagnetic Compatibility (EMC)/Antenns and Propagation (AP) Chapter secretary (2000 and 2001). He was actively involved in organizing the 1999 Asia–Pacific Microwave Conference, Singapore, and was the publication and exhibition chairman of the 1999 Asia–Pacific Microwave Conference, Singapore. He was the recipient of the 1993 URSI Young Scientist Award.